Published in final edited form as:
IEEE J Biomed Health Inform. 2013 March ; 17(2): . doi:10.1109/JBHI.2013.2241071.

Multi-Scale Entropy Analysis of Different Spontaneous Motor Unit Discharge Patterns

Xu Zhang [Member, IEEE],
Sensory Motor Performance Program, Rehabilitation Institute of Chicago, Chicago, IL 60611 USA (xzhang@ric.org)

Xiang Chen [Member, IEEE],
Institute of Biomedical Engineering, University of Science and Technology of China, Hefei, Anhui 230027 China (xch@ustc.edu.cn)

Paul E. Barkhaus, and
Department of Neurology, Medical College of Wisconsin and the Milwaukee Veterans Administration Medical Center, Milwaukee, WI 53295 USA (pbarkhaus@gmail.com)

Ping Zhou [Senior Member, IEEE]
Sensory Motor Performance Program, Rehabilitation Institute of Chicago, Chicago, IL 60611 USA, and with the Department of Physical Medicine and Rehabilitation, Northwestern University, Chicago, IL 60611 USA, and also with the Institute of Biomedical Engineering, University of Science and Technology of China, Hefei, Anhui 230027 China, (p-zhou@northwestern.edu)

Abstract

This study explores a novel application of multi-scale entropy (MSE) analysis for characterizing different patterns of spontaneous electromyogram (EMG) signals including sporadic, tonic and repetitive spontaneous motor unit discharges, and normal surface EMG baseline. Two algorithms for MSE analysis, namely the standard MSE and the intrinsic mode entropy (IMEn) (based on the recently developed multivariate empirical mode decomposition (MEMD) method), were applied to different patterns of spontaneous EMG. Significant differences were observed in multiple scales of the standard MSE and IMEn analyses ($p < 0.001$) for any two of the spontaneous EMG patterns, while such significance may not be observed from the single scale entropy analysis. Compared to the standard MSE, the IMEn analysis facilitates usage of a relatively low scale number to discern entropy difference among various patterns of spontaneous EMG signals. The findings from this study contribute to our understanding of the nonlinear dynamic properties of different spontaneous EMG patterns, which may be related to spinal motoneuron or motor unit health.

Index Terms

Motor unit action potential; multi-scale entropy; spontaneous muscle activity; surface electromyography

I. Introduction

THE presence of spontaneous electromyographic (EMG) activity has been reported in muscles affected by motoneuron diseases (e.g., amyotrophic lateral sclerosis (ALS)) or neurologic disorders (e.g., hemiparetic stroke, spinal cord injury) [1]–[6]. For example,

Color versions of one or more of the figures in this paper are available online at http://ieeexplore.ieee.org.

fibrillation potentials or positive sharp waves and fasciculation potentials have been viewed as evidence of denervation to increase the diagnostic sensitivity of ALS [2]. Spontaneous motor unit activity is also widely present in individuals with spinal cord injury [4], [5] or hemiparetic stroke [6].

In order to quantitatively characterize spontaneous motor unit firing properties, statistics of motor unit firing rates or inter-spike intervals are often used [7]. Recently, we employed approximate entropy (ApEn) measurement to explore the complexity of spontaneous motor unit discharge patterns in ALS [8]. Such entropy analysis [9], [10] serves as a novel approach for evaluating the spontaneous motor unit activity or their neural origins in the nonlinear complexity domain, thus expanding our knowledge of the pathophysiology of motoneuron or motor unit functions.

In recent years, significant advances have been made in entropy analysis. For example, the multiscale entropy (MSE) analysis has been developed which essentially calculates the sample entropy (SampEn) [10] (a robust single scale entropy estimate modified from ApEn [9]) over multiple scales determined by the coarse-grained procedure [11], [12]. Compared with a single entropy measure at the original time scale, the entropy analysis performed over multiple time scales provides more details on the signal dynamics. Taking this advantage, the MSE analysis has achieved a number of applications in assessing the dynamic property of physiological signals in normal controls and disease [11]–[15].

Another recently developed approach, termed intrinsic mode entropy (IMEn) [16], computes SampEn over different scales of time series, namely intrinsic mode functions (IMFs) extracted by empirical mode decomposition (EMD). EMD acts as a fully data-driven method that decomposes a time series into multiple nonlinear scales representing its inherent oscillatory modes. Thus IMEn has been considered as a MSE analysis method adapted to nonstationary and nonlinear nature of physiological time series [17]. Furthermore, extensions of the EMD algorithm such as ensemble EMD (EEMD) [18] and multivariate EMD (MEMD) [19], [20] have been developed to overcome the mode-mixing and mode-misalignment problems of the original EMD algorithm. This makes IMEn analysis a more powerful tool for multi-scale time-frequency analysis of physiological data.

The current study attempts to explore the application of the recent advances in entropy analysis for analyzing different spontaneous EMG patterns. Two MSE algorithms, i.e. the standard MSE and the IMEn analyses were specifically used in this study. Compared with single entropy measurement, the MSE provides more detailed information revealing the nonlinear dynamics of different patterns of spontaneous EMG. This expands our knowledge of generalized spontaneous EMG activity often observed in neuromuscular diseases or neurological disorders.

II. Methods

This section introduces two algorithms for MSE analysis, namely the standard MSE and the recently developed IMEn based on MEMD method, and their application to different spontaneous motor unit patterns recorded from ALS patients.

A. SampEn and Standard MSE

SampEn is an effective and robust entropy measure with a single scale for the short and noisy time series [10]. In order to compute SampEn, a time series (denoted as $x(t)$) is first embedded into a set of vectors in a delayed m-dimensional space. Then, the probability $B^m(r)$ that two vectors match in the m-dimensional space is computed by counting the average number of the matched vector pairs. The match of two vectors is defined as their

distance lower than a tolerance r. Similarly, $B^{m+1}(r)$ can also be computed for the embedded dimension of m+1. Thus, the SampEn is defined as:

$$\mathrm{SampEn}(x, m, r) = -\ln(B^{m+1}(r)/B^{m}(r)). \quad (1)$$

In order to develop MSE analysis, the standard MSE algorithm, which was developed by Costa *et al.* [11], applies the simple "coarse-grained" multiscale approach on the considered time series prior to the entropy measure to determine multiple time scales. In fact, the "coarse-grained" approach represents a linear smoothing that gradually removes the fine-scale (high-frequency) components of the original time series. Thus, the standard MSE is obtained by computing SampEn over these scales.

B. MEMD-based IMEn

Algorithms for computing the standard EMD and its modified version, MEMD, have been previously provided in detail [19], [20]. Amoud et al. [16] first defined the calculation of IMEn based on standard EMD. Hu and Liang [21], [22] further refined the MEMD-based IMEn analysis method. Here, we present a brief summary of these calculations, slightly modified from their description [21].

The EMD is a fully adaptive, data-driven method that is able to decompose a time-series, by the sifting algorithm, into a finite set of IMFs. These represent the inherent oscillation modes of that time series [17]. The EMD performed prior to entropy analysis, referred to as the IMEn analysis, enables entropy to be calculated over different scales of the original time series. The EMD-based IMEn analysis thus becomes an investigatory approach for the characterization of univariate time series. However, the mode-misalignment introduced by standard EMD limits its further application on the multivariate time series data. Recently, MEMD [19], [20] has been proposed to extend the application of the EMD technique to multivariate data, thus inspiring the improved IMEn analysis based on the MEMD [21], [22].

The key to the MEMD algorithm is the calculation of the local mean. In EMD, the local mean is computed by taking an average of upper and lower envelopes obtained by interpolating the local maxima and minima of the signal. MEMD works directly with multivariate data (usually representing n-variable time series) in which the local maxima and minima are not well defined. To deal with this problem, multiple n-dimensional envelopes are generated by taking signal projections along different directions in (n−1)-dimensional spaces. These envelopes are then averaged to obtain the local mean. Considering that $\{\mathbf{v}(t)\}_{t=1}^{T}$ is an input time series in an n-variable form, and $\mathbf{x}^{\theta_k}$ denotes a set of vectors along the directions represented by angles $\theta_k = \{\theta_1^k, \theta_2^k, \ldots, \theta_{n-1}^k\}$ on the (n−1)-sphere, the algorithm can be briefly summarized as follows [19]:

1. Generate a point set based on the Hammersley sequence for sampling on an (n−1)-sphere.
2. Calculate a projection $p^{\theta_k}(t)\}_{t=1}^{T}$ of the multivariate input data $\{\mathbf{v}(t)\}_{t=1}^{T}$ along a direction vector $\mathbf{x}^{\theta_k}$, for all k, thus giving $p^{\theta_k}(t)\}_{k=1}^{K}$ as the set of projections.
3. Locate the time points $t_i^{\theta_k}$ according to maxima of the set of projected signal $p^{\theta_k}(t)\}_{k=1}^{K}$.

4. Interpolate $\left[t_i^{\theta_k}, \mathbf{v}(t_i^{\theta_k})\right]$, for all values of k, to obtain multivariate envelope curves $\mathbf{e}^{\theta_k}(t)\}_{k=1}^{K}$.
5. For a set of K direction vectors, calculate the mean $\mathbf{m}(t)$ of the envelop curves

$$\mathbf{m}(t)=(1/K)\sum_{k=1}^{K}\mathbf{e}^{\theta_k}(t). \quad (2)$$

6. Iterate on the detail $\mathbf{d}(t) = \mathbf{v}(t) - \mathbf{m}(t)$ until it becomes a multivariate IMF. The above procedure is then applied to $\mathbf{v}(t) - \mathbf{d}(t)$.

The stoppage criterion for multivariate IMFs is similar to that for the univariate IMFs except that the equality constraint for the number of extrema and zero crossings is not imposed, as extrema cannot be properly defined for the multivariate signal [19]. By projection, MEMD directly processes the multivariate signal to produce the mode-aligned IMFs.

The mode alignment of resultant IMFs derived from MEMD allows two IMEn algorithms, namely the fine-to-coarse IMEn and the coarse-to-fine IMEn, which indicate that the multiple scales can be determined in a way of consecutively removing either the high-frequency or low-frequency IMFs from the original data [21]. Note that the standard MSE can be regarded as a fine-to-coarse approach.

The calculation of fine-to-coarse IMEn based on MEMD is the same as the standard IMEn based on EMD. The fine-to-coarse IMEn is the SampEn computed over the adaptive scales selected by removing the high-frequency IMFs, starting from the first IMF,

$$\mathrm{IMEn}_{f2c}(k,m,r)=\mathrm{SampEn}(S_{f2c}^{k},m,r), \quad (3)$$

where the fine-to-coarse scale S_{f2c}^{k} is defined as $S_{f2c}^{k}=\sum_{i=k}^{N}\mathrm{IMF}_i, k \leq N$. Here, N represents the total number of IMFs, where the residual is always regarded as the last IMF, in this study. On the other hand, the coarse-to-fine IMEn can be calculated by consecutively removing the low-frequency IMFs, starting from the last IMF (e.g. the residual),

$$\mathrm{IMEn}_{c2f}(k,m,r)=\mathrm{SampEn}(S_{c2f}^{k},m,r), \quad (4)$$

where the coarse-to-fine scale S_{c2f}^{k} is defined as $S_{c2f}^{k}=\sum_{i=1}^{N+1-k}\mathrm{IMF}_i, k \leq N$.

In this study, the parameters m and r in the calculation of SampEn were chosen as 2 and 0.15×SD, the standard deviation of the processed signal segment, respectively, to minimize the standard error of entropy estimation [23].

C. Processed Dataset Description

The dataset used in this study was selected from spontaneous EMG recordings of 9 subjects (six males, three females, 57 ± 7 years) with “Definite ALS” or “Probable ALS with Laboratory Support”. The study was approved by the local Institutional Review Board. During the data collection, each subject was positioned comfortably supine on a clinical bed in a quiet examination room without any disturbing sensory stimuli. The spontaneous surface EMG signals were recorded bilaterally from the thenar muscle while the tested arm was placed in its resting position. A Refa system (TMS International, Enschede, The Netherlands) comprising a 128-channel amplifier and a flexible surface electrode array with 64 (in an 8 × 8 square formation) recording probes (1.2 mm diameter, 4 mm inter-electrode

distance) was used for data collection. The system built-in band-pass filter was set at 20–500 Hz, and all recorded surface EMG signals were sampled at 2 kHz per channel. The duration of each spontaneous muscle activity recording from ALS subjects lasted at least 4 minutes.

From the spontaneous surface EMG recordings of the ALS subjects, three types of spontaneous action potentials were selected from the database in term of their firing patterns. One type represented the sporadic spikes firing randomly at very low firing rates. The other type always exhibited a series of spikes firing regularly, which was similar to a motor unit action potential at minimal activation. The third type represented high-frequency, repetitive action potential discharges, such as doublets, triplets, multiplets, or prolonged iterative spontaneous discharges (i.e. myokymic or neuromyotonic discharges). In contrast to the different spontaneous EMG patterns from the ALS database, a normal spontaneous EMG with quiescent baseline recordings was also reviewed, using data collected from 9 healthy control subjects. For each type of the three spontaneous EMG patterns and the normal surface EMG baseline pattern, 25 representative data segments (each 500ms in length) were selected from the database, generating 100 signal segments in total. A data segment length of 500 ms was expected to be adequate to show distinct information regarding the general firing rate and action potential duration of the considered spontaneous EMG patterns. A longer length segment might contain too much background noise, whereas a shorter one might not sufficiently reveal patterns having multiple discharges.

D. Data Processing

All of the selected 100 signal segments were reshaped into a multivariate form as a 100-dimensional dataset which was suitable for MEMD analysis. The source code for MEMD, which is publicly available from the webpage of MEMD algorithm's proposer [32], was exploited for fast and convenient implementation of this algorithm in Matlab (version 2012a, The Mathworks Inc., MA) environment. Since the number of directions is suggested to be considerably greater than the dimension of multivariate signals [32], we set the number of directions at 512 for MEMD implementation. The resultant scale-aligned IMFs for each signal segment were obtained at the same time. Both the fine-to-coarse and coarse-to-fine IMEn analyses were then performed over multiple scales interpreted by the consecutive summation of a part of IMFs along different ways. The standard MSE results were also computed for each signal segment for comparison purpose. A one-way analysis of variance (ANOVA) was performed to examine the effect of entropy measure across multiple scales on the discrimination of different spontaneous EMG patterns. The level for significance was set to 0.001.

III. Results

A. Standard MSE Analysis

The standard MSE was performed on each of the selected segments of spontaneous EMG signals. Fig. 1 shows the results of MSE (averaged from 25 segments for each spontaneous EMG pattern) as a function of scale factor used in the coarse-grained procedure. It was found that at all scale factors, the MSE curve for normal surface EMG baselines (indicated as the healthy pattern) was above the curves for the other three patterns with its entropy values varying approximately from 1.5 to 2.4. The MSE curve for the repetitive pattern was below the other three patterns with its entropy values lower than 0.5, which were relatively consistent with the entropy values at the original scale. The MSE curves for the sporadic and tonic patterns exhibited a similar trend that entropy increased at scale factors below 6, then maintained relatively stable or slightly decreased at scale factors higher than 6. At the scale factors from 6 to 14, there was a significant difference ($p < 0.001$) between any two of the four spontaneous EMG patterns.

B. MEMD-based IMEn Analysis

Fig. 2 shows the corresponding IMFs for each of the representative signal segments for the three spontaneous EMG patterns. It can be observed that the IMFs with the same scale index exhibited a similar common oscillation mode across all the signal segments.

After applying the MEMD method on the entire spontaneous EMG dataset reshaped into multivariate form, the aligned IMFs across all signal segments were obtained. Then, the IMEn analysis could be performed over the obtained scales. Fig. 3 shows the coarse-to-fine IMEn results averaged from 25 selected segments for each of the four different spontaneous EMG patterns. For scale one (the original scale), the healthy pattern and the repetitive pattern demonstrated the highest and lowest entropy values, respectively ($p < 0.001$ for either the healthy or repetitive pattern vs. any of the others), and the entropy values for the sporadic and tonic patterns partly overlapped ($p = 0.002$). As the fine-scale IMFs were progressively removed from the raw signal segment, entropy values for all four patterns generally exhibited a decreasing trend but with different decreasing rates. With relatively high scales, the entropy for the healthy pattern dropped most rapidly, and the IMEn values for the sporadic and tonic patterns were likely to be separate. Across all segments selected from the spontaneous EMG database, it was found that a significant difference between any two of the four patterns occurred at the 4th scale ($p < 0.001$). The tonic pattern could be mostly distinguished from the sporadic and repetitive patterns ($p < 0.001$) at the 5th scale while its entropy overlapped with the healthy pattern at this scale ($p = 0.008$).

The coarse-to-fine IMEn results for the same selected 100 segments are shown in Fig. 4. Across the examined signals, it was observed that the entropy value for each pattern did not vary significantly as the coarse-scale IMFs were gradually discarded. The resultant IMEn curves for each pattern were stable from the 1st to 7th scale and then started to decrease from the 8th scale. No significant difference could be observed between the sporadic and tonic patterns at any scale ($p > 0.001$).

IV. Discussions and Conclusion

The nonlinear dynamic properties of surface EMG signals have been examined with different entropy algorithms [24]–[30]. Compared with the single scale entropy, the MSE analysis has been proved to be a more suitable approach in quantifying the degree of complexity of physiological signals having multiple spatiotemporal scales [11]–[15]. In this study, two MSE algorithms, i.e. the standard MSE and the MEMD based IMEn, were used to characterize the spontaneous EMG patterns often observed in diseased muscles.

Across almost all scales, the normal surface EMG baseline (or the healthy pattern) yielded the highest entropy values over the other three spontaneous EMG patterns. This indicates that the normal surface EMG baselines are more complex and irregular than the spontaneous sporadic, tonic or repetitive spikes. This observation is in accordance with the general hypothesis proposed in the medical sciences [31] that abnormal physiology is always associated with more regularity. Similarly, the repetitive spikes showed the lowest entropy values over all scales, suggesting that they have the lowest complexity level and contain the least information among different spontaneous EMG patterns.

When only the original time scale (raw data) was considered, the repetitive spontaneous spikes and the normal surface EMG baseline can be easily discriminated from others by their lowest and highest mean entropy values, respectively. This was consistent with the findings of our previous study using the single-scale entropy analysis [8]. However, the sporadic and tonic discharge patterns may have overlapping entropy values at the original scale. By contrast, when calculating entropy that takes into account different time scales of

the time series, the resultant dynamic entropy curves could illustrate valid differences between different spontaneous EMG patterns. This may enhance discrimination capacity.

With the current dataset, the MEMD method synchronously yielded 10 aligned IMFs (scales), and the fine-to-coarse IMEn analysis exhibited significant differences between the four patterns at scale 4. In contrast, the standard MSE analysis had to be performed over more scales (larger than 6) in order to discern such a significant difference. The relative small scale number required by the IMEn analysis may be due to the adaptive multiscale approach of the EMD, where there is nonlinear selection of scales according to the processed signal characteristics [16], [18]–[21]. In contrast, the coarse-grained procedure used for standard MSE is purely linear. The advantage provided by the EMD family methods makes IMEn more appropriate in characterizing the dynamics of the physiological signals, as compared to the standard MSE.

Another advantage of MEMD-based IMEn analysis is that the scale-aligned IMFs derived from the MEMD allow not only fine-to-coarse but also coarse-to-fine IMEn analysis [21]. The coarse-to-fine IMEn analysis illustrated a steady entropy curve for each discharge pattern in scales 1 to 7, indicating that the entropy has relative dependence on fine-scale (high-frequency) components in the spontaneous EMG. The rationale behind this observation was that all the selected surface EMG recordings had a quiescent baseline, and thereby the amplitude of their coarse-scale (low-frequency) components was very low, as indicated by the high order IMFs in Fig. 2. By comparing the fine-to-coarse and coarse-to-fine IMEn results, we can infer that the first 5 IMFs (representing the high-frequency components) contain the most distinguishing features of the signal dynamics for discrimination between different spontaneous EMG patterns.

The mean SampEn value of the tonic spikes was slightly lower than that of the sporadic spikes at the original scale. However, the tonic spikes yielded significantly higher SampEn values than the sporadic spikes at larger scales, indicating that the tonic spikes had higher complexity level and contained more information than the sporadic spikes. This observation revealed by the MSE analysis supplements our previous findings using single-scale entropy analysis [8]. More specifically, with the fine-to-coarse IMEn analysis (Fig. 3) and the standard MSE analysis (Fig. 1), the entropy curve of tonic spikes started below but exceeded that of sporadic spikes as the scale factor increased. The relative increase in complexity of the tonic spikes compared with the sporadic spikes implies the long-range variability in the tonic dynamics due to the inherent changes of firing properties over time.

It should be noted that this study focuses on the MSE analysis of different spontaneous motor unit discharge patterns. The results were obtained from 100 signal segments (500 ms in duration) selected from the spontaneous EMG database (with 25 segments representing each of the spontaneous motor unit discharge patterns). Our objective was not, however, to compare the complexity of spontaneous EMG between ALS and neurologically intact subjects or between different subjects. For a specific subject, we acknowledge that there are many other factors (e.g., signal segment selection, segment duration, EMG channel, etc.) that may influence the MSE analyses, and these factors must be considered when different subjects are to be compared.

In conclusion, MSE analyses including the standard MSE and the MEMD-based IMEn were performed in this study to characterize the dynamics of different spontaneous EMG patterns. Both methods offered a distinctive description for different patterns in terms of their complexity changing over multiple time scales. Significant differences between any two spontaneous EMG patterns were observed in multiple scales of the standard MSE and the IMEn analyses, while such significance may not be observed from the single scale entropy

analysis. Furthermore, taking advantage of the MEMD that adaptively decomposes multivariate time series into a finite set of mode-aligned IMFs, the IMEn analysis required a relatively low scale number compared to the standard MSE to discern significant differences among different spontaneous EMG signals. These findings from the MSE analysis expand our understanding of the nonlinear dynamic properties of different spontaneous EMG patterns, which may be related to the spinal motoneuron or motor unit's integrity.

Acknowledgments

The authors thank Faezeh Jahanmiri-Nezhad, M.S. and Xiaoyan Li, Ph.D. for their help with data collection.

This work was supported in part by the National Institute on Disability and Rehabilitation Research of the U.S. Department of Education under Grant H133G090093, in part by the National Institutes of Health of the U.S. Department of Health and Human Services under Grant R21NS075463 and Grant R24HD050821.

References

1. de Carvalho M, Dengler R, Eisen A, England JD, Kaji R, Kimura J, Mills K, Mitsumoto H, Nodera H, Shefner J, Swash M. Electrodiagnostic criteria for diagnosis of ALS. Clin. Neurophysiol. 2008 Mar.vol. 119(no. 3):497–503. [PubMed: 18164242]
2. Noto YI, Misawa S, Kanai K, Shibuya K, Isose S, Nasu S, Sekiguchi Y, Fujimaki Y, Nakagawa M, Kuwabara S. Awaji ALS criteria increase the diagnostic sensitivity in patients with bulbar onset. Clin. Neurophysiol. 2012 Feb.vol. 123(no. 2):382–385. [PubMed: 21764635]
3. Valls-Solé J, Montero J. Role of EMG evaluation in muscle hyperactivity syndromes. J. Neurol. 2004 Mar.vol. 251(no. 3):251–260. [PubMed: 15015003]
4. Thomas CK, Ross BH. Distinct patterns of motor unit behavior during muscle spasms in spinal cord injured subjects. J. Neurophysiol. 1997 May; vol. 77(no. 5):2847–2850. [PubMed: 9163400]
5. Wallace DM, Ross BH, Thomas CK. Characteristics of lower extremity clonus after human cervical spinal cord injury. J. Neurotrauma. 2012 Mar.vol. 29(no. 5):915–924. [PubMed: 21910643]
6. Mottram CJ, Suresh NL, Heckman CJ, Gorassini MA, Rymer WZ. Origins of abnormal excitability in biceps brachii motoneurons of spastic-paretic stroke survivors. J. Neurophysiol. 2009 Jul.vol. 102(no. 4):2026–2038. [PubMed: 19587321]
7. Kleine BU, Stegeman DF, Schelhaas HJ, Zwarts MJ. Firing pattern of fasciculations in ALS: evidence for axonal and neuronal origin. Neurology. 2008 Jan.vol. 70(no. 5):353–359. [PubMed: 18227416]
8. Zhou P, Barkhaus PE, Zhang X, Rymer WZ. Characterizing the complexity of spontaneous motor unit patterns of amyotrophic lateral sclerosis using approximate entropy. J. Neural Eng. 2011 Dec.vol. 8(no. 6) p. 066010.
9. Pincus SM. Approximate entropy as a measure of system complexity. Proc. Natl. Acad. Sci. U.S.A. 1991 Mar.vol. 88(no. 6):2297–2301. [PubMed: 11607165]
10. Richman JS, Moorman JR. Physiological time-series analysis using approximate entropy and sample entropy. Am. J. Physiol. (Heart Circ. Physiol.). 2000 Jun.vol. 278(no. 6):H2039–H2049. [PubMed: 10843903]
11. Costa M, Goldberger AL, Peng C-K. Multiscale entropy analysis of complex physiologic time series. Phys. Rev. Lett. 2002 Aug.vol. 89(no. 6) p. 068102.
12. Costa M, Healey JA. Multiscale entropy analysis of complex heart rate dynamics: discrimination of age and heart failure effects. Computers in Cardiology. 2003:705–708.
13. Ferrario M, Signorini MG, Magenes G, Cerutti S. Comparison of entropy-based regularity estimators: application to the fetal heart rate signal for the identification of fetal distress. IEEE Trans. Biomed. Eng. 2006 Jan.vol. 53(no. 1):119–125. [PubMed: 16402611]
14. Wu HT, Hsu PC, Lin CF, Wang HJ, Sun CK, Liu AB, Lo MT, Tang CJ. Multiscale entropy analysis of pulse wave velocity for assessing atherosclerosis in the aged and diabetic. IEEE Trans. Biomed. Eng. 2011 Oct.vol. 58(no. 10):2978–2981. [PubMed: 21693413]

15. Humeau A, Mahe G, Chapeau-Blondeau F, Rousseau D, Abraham P. Multiscale analysis of microvascular blood flow: a multiscale entropy study of laser Doppler flowmetry time series. IEEE Trans. Biomed. Eng. 2011 Oct.vol.58(no.10):2970–2973. [PubMed: 21712149]
16. Amoud H, Snoussi H, Hewson D, Doussot M, Duchêne J. Intrinsic Mode Entropy for Nonlinear Discriminant Analysis. IEEE Signal Process. Lett. 2007 May; vol. 14(no. 5):297–300.
17. Huang NE, Shen Z, Long SR, Wu ML, Shih HH, Zheng Q, Yen NC, Tung CC, Liu HH. The empirical mode decomposition and Hilbert spectrum for nonlinear and nonstationary time series analysis. Proc. Roy. Soc. Amer. 1998; vol. 454:903–995.
18. Wu Z, Huang NE. Ensemble empirical mode decomposition: A noise-assisted data analysis method. Adv. Adapt. Data Anal. 2009 Jan.vol. 1(no. 1):1–41.
19. Rehman N, Mandic DP. Multivariate empirical mode decomposition. Proc. Roy. Soc. Amer. 2010; vol. 466:1291–1302.
20. Rehman N, Mandic DP. Filter Bank Property of Multivariate empirical mode decomposition. IEEE Trans. Signal Process. 2011 May; vol. 59(no. 5):2421–2426.
21. Hu M, Liang H. Adaptive multiscale entropy analysis of multivariate neural data. IEEE Trans. Biomed. Eng. 2012 Jan.vol.59(no.1):12–15. [PubMed: 21788182]
22. Hu M, Liang H. Intrinsic mode entropy based on multivariate empirical mode decomposition and its application to neural data analysis. Cogn. Neurodyn. 2011 Sep.vol. 5(no. 3):277–284. [PubMed: 22942916]
23. Lake D, Richman J, Griffin M, Moorman J. Sample entropy analysis of neonatal heart rate variability. Am. J. Physiol. (Regulatory Integrative Comp. Physiol.). 2002 Sep.vol. 283:R789–R797.
24. Xie HB, Guo JY, Zheng YP. Fuzzy approximate entropy analysis of chaotic and natural complex systems: detecting muscle fatigue using electromyography signals. Ann. Biomed. Eng. 2010 Apr.vol. 38(no. 4):1483–1496. [PubMed: 20099031]
25. Istenic R, Kaplanis PA, Pattichis CS, Zazula D. Multiscale entropy-based approach to automated surface EMG classification of neuromuscular disorders. Med. Biol. Eng. Comput. 2010 Aug.vol. 48(no. 8):773–781. [PubMed: 20490940]
26. Ahmad SA, Chappell PH. Surface EMG pattern analysis of the wrist muscles at different speeds of contraction. J. Med. Eng. Technol. 2009; vol. 33(no. 5):376–385. [PubMed: 19440916]
27. Kosmidou VE, Hadjileontiadis LJ. Sign language recognition using intrinsic-mode sample entropy on sEMG and accelerometer data. IEEE Trans. Biomed. Eng. 2009 Dec.vol. 56(no. 12):2879–2890. [PubMed: 19174329]
28. Chen W, Wang Z, Xie H, Yu W. Characterization of surface EMG signal based on fuzzy entropy. IEEE Trans. Neural Syst. Rehabil. Eng. 2007 Jun.vol. 15(no. 2):266–272. [PubMed: 17601197]
29. Akkurt D, Akay YM, Akay M. The effects of elevated body temperature on the complexity of the diaphragm EMG signals during maturation. J. Neural Eng. 2009 Apr.vol. 6(no. 2) p. 024001.
30. Dragomir A, Akay Y, Curran AK, Akay M. Complexity measures of the central respiratory networks during wakefulness and sleep. J. Neural Eng. 2008 Jun.vol. 5(no. 2):254–261. [PubMed: 18506077]
31. Pincus SM, Goldberger AL. Physiological time-series analysis: what does regularity quantify? Am. J. Physiol. (Heart Circ. Physiol.). 1994 Apr.vol. 266(no. 4):H1643–H1656.
32. Rehman, N.; Mandic, DP. 2010. http://www.commsp.ee.ic.ac.uk/~mandic/research/emd.htm

Biographies

Xu Zhang (M'11) received his B.S. degree in electronic information science and technology and Ph.D. degree in biomedical engineering from University of Science and Technology of China, Hefei, China, in 2005 and 2010, respectively.

He is currently a postdoctoral fellow at the Rehabilitation Institute of Chicago, Chicago, IL, USA. His research interests include biomedical signal processing, pattern recognition, pathophysiology in neuromuscular disorders and neurorehabilitation engineering.

Xiang Chen (M'11) received her M.S. and Ph.D. degree in biomedical engineering from University of Science and Technology of China, Hefei, China, in 2000 and 2004, respectively.

From 2001 to 2008, she was an instructor in the Department of Electronic Science and Technology, University of Science and Technology of China, where she has been an Associate Professor since 2008. She is currently the director of the Neural Muscular Control Laboratory of the Institute of Biomedical Engineering at University of Science and Technology of China. Her research interests include biomedical signal processing, multi-modal user interfaces and mobile healthcare.

Paul E. Barkhaus received his B.S. and M.D. degrees from Wayne State University in Detroit, MI. He completed his training in neurology at Wayne State University in 1978, followed by fellowships in clinical neuromuscular diseases at the University of Arizona and two fellowships in Electromyography at the University of Minnesota and Duke University.

Dr. Barkhaus has been on faculty at the Medical College of Wisconsin since 1993. He was appointed Professor of Neurology in 2002, and awarded tenure in 2011. He developed the Amyotrophic Lateral Sclerosis (Lou Gehrig Disease) Program in the late 1990's and it is currently one of almost 40 centers of the ALS Association's Centers of Excellence in the USA. Dr. Barkhaus also serves as the Department of Neurology's Program Director for Clinical neurophysiology and is Section Chief for Neuromuscular and Autonomic Disorders. His current research interests are in clinical neurophysiology (electromyography and electroneurography) and amyotrophic lateral sclerosis.

Ping Zhou (S'01–M'05–SM'07) received the B.S. degree in electrical engineering and the M.S. degree in biomedical engineering from the University of Science and Technology of

China, Hefei, China, in 1995 and 1999, respectively, and the Ph.D. degree in biomedical engineering from Northwestern University, Evanston, IL, in 2004. His Ph.D. dissertation project was performed as part of the Sensory Motor Performance Program (SMPP), Rehabilitation Institute of Chicago, Chicago, IL, USA.

From 2004 to 2006, he was a Research Associate in the Neural Engineering Center for Artificial Limbs (NECAL), Rehabilitation Institute of Chicago. After that he has been a Research Scientist in NECAL and later in SMPP at the Rehabilitation Institute of Chicago. He has been an Adjunct Assistant Professor since 2006 in the Department of Physical Medicine and Rehabilitation, Northwestern University, Chicago, USA, and a Professor since 2012 in the Institute of Biomedical Engineering, University of Science and Technology of China, Hefei, China. His current research interests include biomedical signal (in particular, EMG) processing, motor unit pathophysiology, noninvasive electrodiagnosis of neuromuscular diseases, computational modeling of neuromuscular systems, myoelectric prosthesis control, and assistive devices for neurorehabilitation.

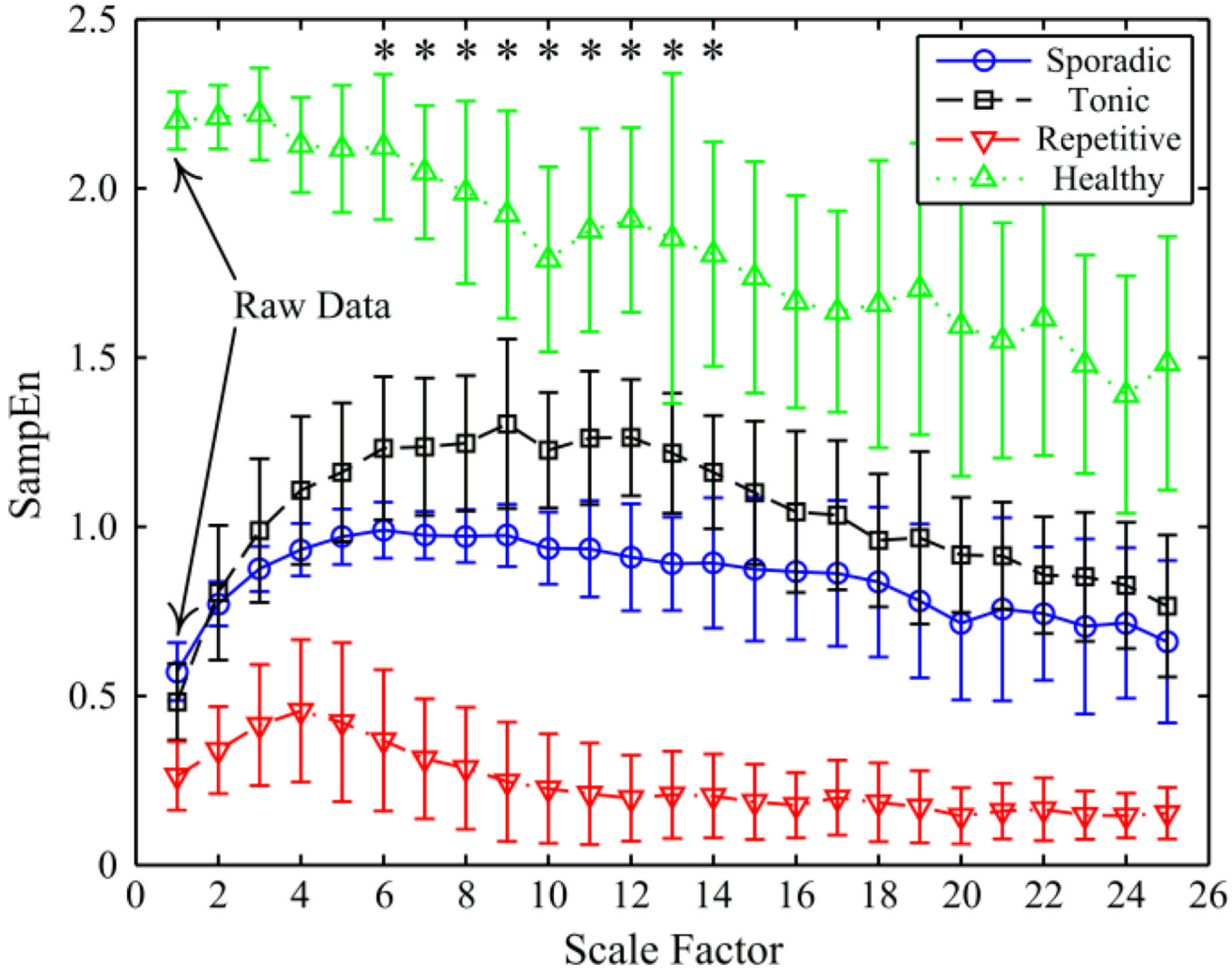

Fig. 1.

The standard MSE results for the four different spontaneous EMG patterns. Error bars refer to the standard deviation of the entropy value averaged across all signal segments for each pattern. The asterisk sign "*" represents significant difference between any two of the four patterns.

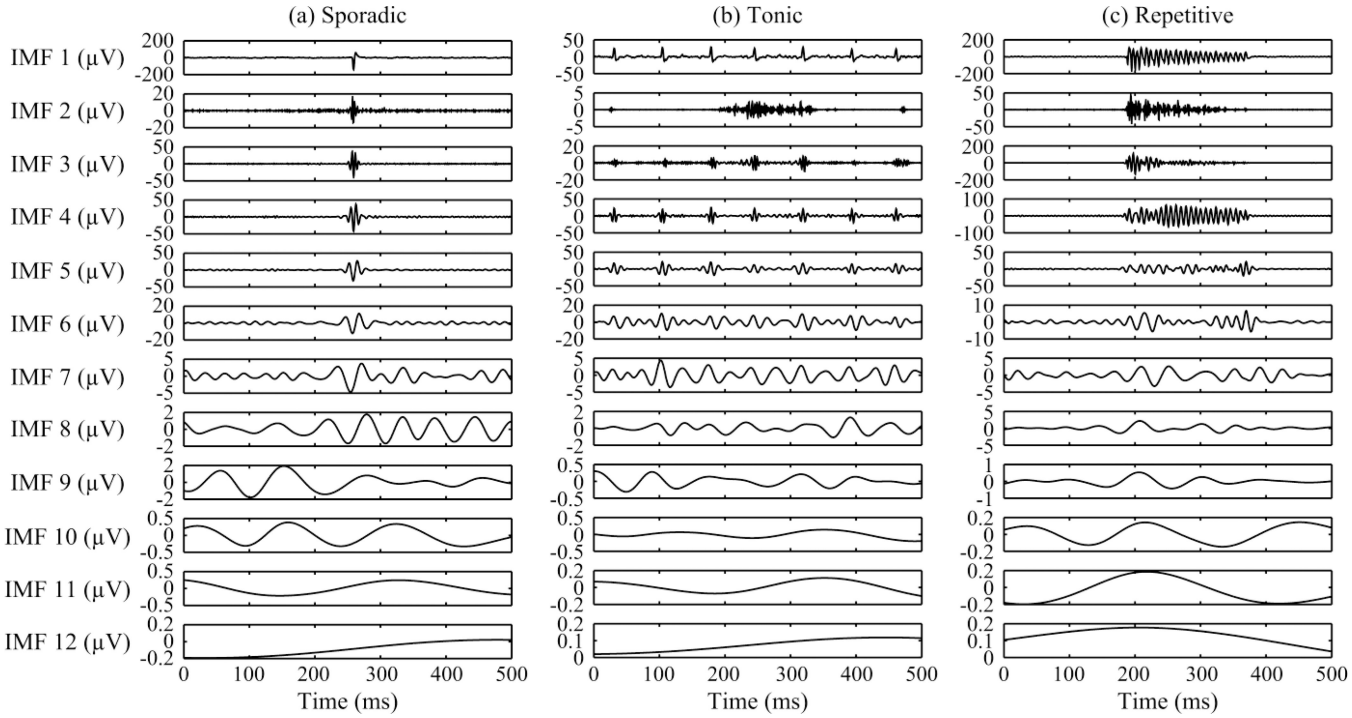

Fig. 2.

Examples of representative signal segments for three distinct spontaneous EMG patterns: (a) sporadic discharge, (b) tonic discharge, and (c) repetitive discharge, and their corresponding IMFs after the MEMD.

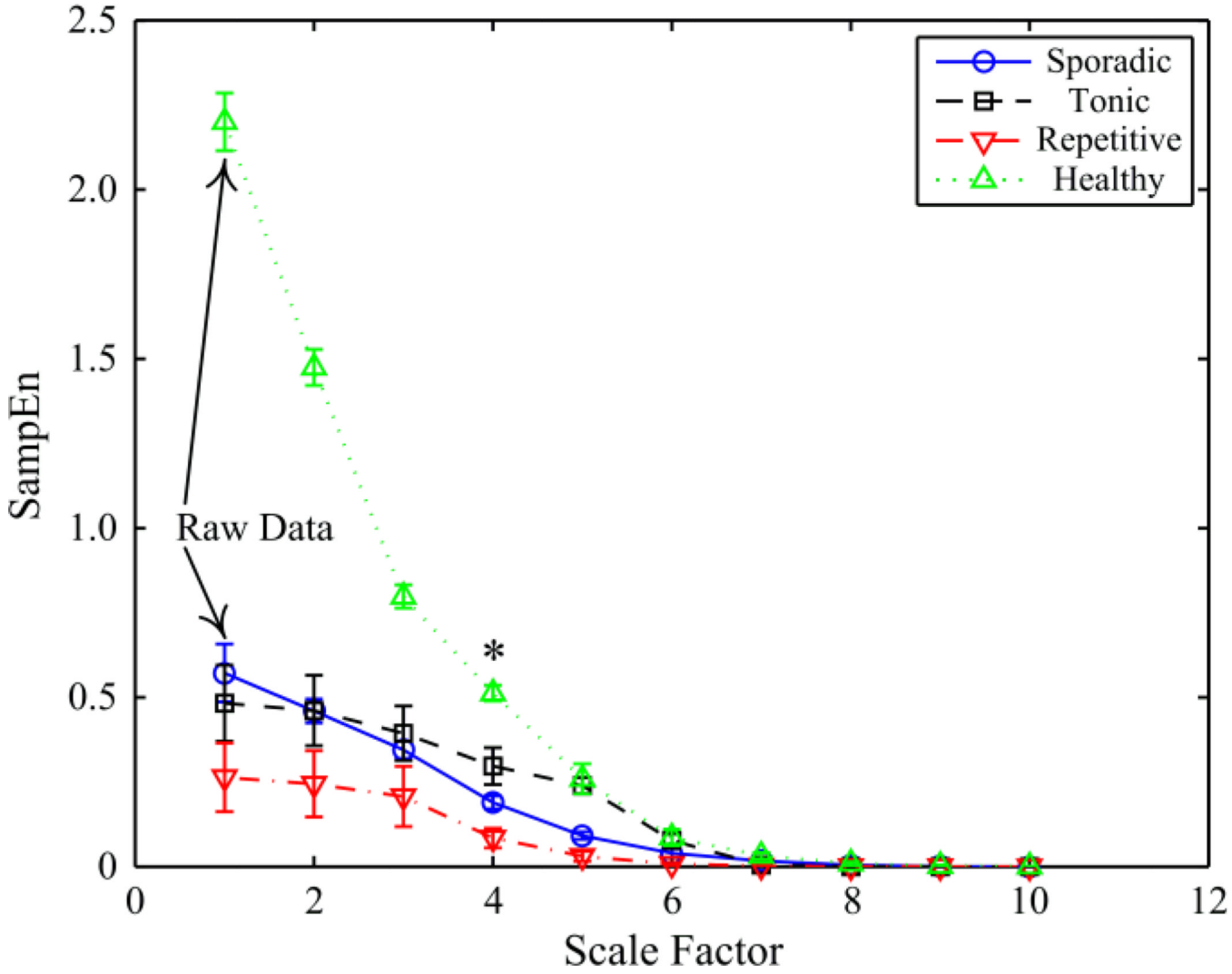

Fig. 3.

MEMD-based fine-to-coarse IMEn results for the four different spontaneous EMG patterns. Error bars refer to the standard deviation of the entropy value averaged across all signal segments for each pattern.

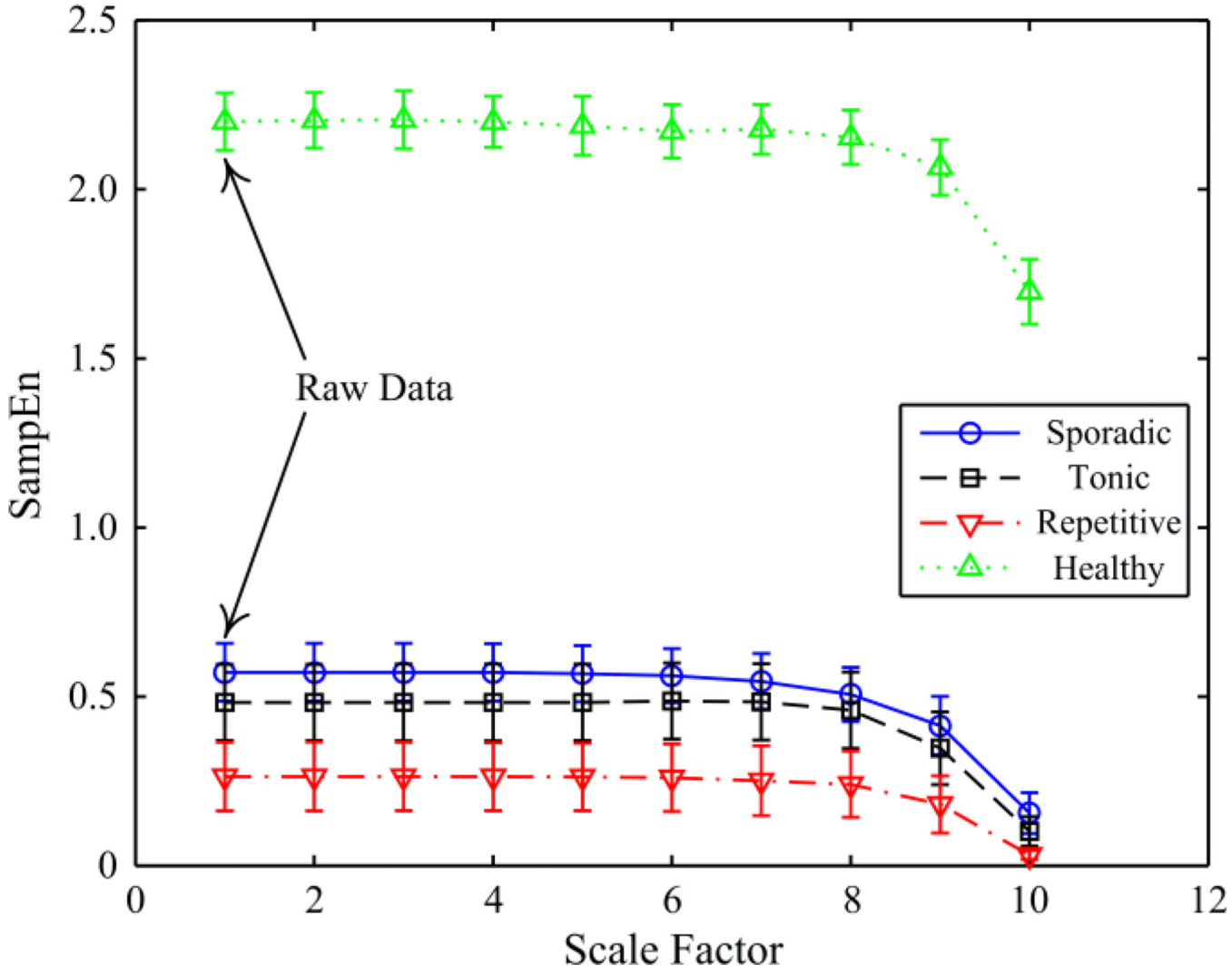

Fig. 4.

MEMD-based coarse-to-fine IMEn results for the four different spontaneous EMG patterns. Error bars refer to the standard deviation of the entropy value averaged across all signal segments for each pattern.